Apparent ecosystem carbon turnover time: uncertainties and robust features

Naixin Fan[1], Sujan Koirala[1], Markus Reichstein[1], Martin Thurner[3], Valerio Avitabile[4], Maurizio Santoro[5], Bernhard Ahrens[1], Ulrich Weber[1], Nuno Carvalhais[1,2]

[1]Max Planck Institute for Biogeochemistry, Hans Knöll Strasse 10, 07745 Jena, Germany

[2]Departamento de Ciências e Engenharia do Ambiente, DCEA, Faculdade de Ciências e Tecnologia, FCT, Universidade Nova de Lisboa, 2829-516 Caparica, Portugal

[3]Biodiversity and Climate Research Centre (BiK-F), Senckenberg Gesellschaft für Naturforschung, Senckenberganlage 25, 60325 Frankfurt am Main, Germany

[4]European Commission, Joint Research Centre, Via E. Fermi 2749, 21027 Ispra, Italy

[5]Gamma Remote Sensing, 3073 Gümligen, Switzerland

Correspondence to: Naixin Fan (nfan@bgc-jena.mpg.de) and Nuno Carvalhais (ncarval@bgc-jena.mpg.de)

Abstract. The turnover time of terrestrial carbon (τ) controls the global carbon cycle – climate feedback and, yet, is poorly simulated by the current Earth System Models (ESMs). In this study, by assessing apparent carbon turnover time as the ratio between carbon stocks and fluxes, we provide a new, updated ensemble of diagnostic terrestrial carbon turnover times and associated uncertainties on a global scale using multiple, state-of-the-art, observation-based datasets of soil organic carbon stock (C_{soil}), vegetation biomass (C_{veg}) and gross primary productivity (GPP). Using this new ensemble, we estimated the global average τ to be 42^{+9}_{-5} years when the full soil depth is considered, longer than the previous estimates of 23^{+7}_{-4} years. Only considering the top 1 m (assuming maximum active layer depth is up to 1 meter) of soil carbon in circumpolar regions yields a global τ of 35^{+9}_{-4} years. C_{soil} in circumpolar regions account for two thirds of the total uncertainty in global τ estimates, whereas C_{soil} in non-circumpolar contributes merely 9.38%. GPP (2.25%) and C_{veg} (0.05%) contribute even less to the total uncertainty. Therefore, the high uncertainty in C_{soil} is the main factor behind the uncertainty in global τ, as reflected in the larger range of full-depth C_{soil} (3152-4372 PgC). The uncertainty is especially high in circumpolar regions with a uncertainty of 50% and the spatial correlations among different datasets are also low compared to other regions. Overall, we argue that current global datasets do not support robust estimates of τ globally, for which we need clarification on variations of C_{soil} with soil depth and stronger estimates of C_{soil} in circumpolar regions. Despite the large variation in both magnitude and spatial patterns of τ, we identified robust features in the spatial patterns of τ that emerge regardless of soil depth and differences in data sources of C_{soil}, C_{veg} and GPP. Our findings show that the latitudinal gradients of τ are consistent across different datasets and soil depth. Furthermore, there is a strong consensus on the negative correlation between τ and temperature along latitude that is stronger in temperate zones (30ºN-60ºN) than in subtropical and tropical zones (30ºS-30ºN). The identified robust patterns can be used to infer the response of τ to climate and for constraining contemporaneous

behaviour of ESMs which could contribute to uncertainty reductions in future projections of the carbon cycle - climate
feedback. The dataset of the terrestrial turnover time ensemble (DOI: 10.17871/bgitau.201911) is openly available from the
35   data portal: https://doi.org/10.17871/bgitau.201911 (Fan et al., 2019).

1 Introduction

Terrestrial carbon turnover time (τ) is the average time that carbon atoms spend in terrestrial ecosystems from initial
photosynthetic fixation until respiratory or non-respiratory loss (Bolin and Rodhe, 1973; Barrett, 2002; Carvalhais et al.,
2014). It is an emergent property that can better represent the macro-scale turnover rate of terrestrial carbon that emerges
40   from different processes such as plant mortality and soil decomposition. Alongside photosynthetic fixation of carbon, τ is a
critical ecosystem property that co-determines the terrestrial carbon storage and the carbon sink potential. As a result of the
balance between inputs and outputs of carbon, the terrestrial carbon pool can be approximated to reach the steady-state
condition (inputs equal outputs) when long timescales are considered. This simplifies the calculation of τ to the ratio between
the total terrestrial carbon storage and the influx or the outflux of carbon. The approach is advantageous to represent the
45   highly heterogeneous intrinsic properties of the terrestrial carbon cycle as an averaged apparent ecosystem property which is
more intuitive to infer large scale sensitivity of τ to climate change. Instead of focusing on the heterogeneity of individual
compartment turnover times we show the change of carbon cycle on the ecosystem level using τ as an emergent diagnostic
property.

The magnitude of τ and its sensitivity to climate change is central to modelling carbon cycle dynamics. Therefore, τ has been
50   used as an emergent ecosystem property to evaluate and constrain Earth system model (ESM) simulations of the carbon
cycle. The current ensemble of ESMs shows a large spread in the simulation of soil carbon stocks and its spatial distribution,
mostly attributed to the differences in τ among ESMs (Friend et al., 2014; Todd-Brown, 2013,2014; Wenzel, et al., 2014,
Carvalhais et al. 2014; Thurner et al., 2017). Thus, it is instrumental to have an observational-based estimation of carbon
turnover times and their associated uncertainty in order to constrain the models and better predict the response of carbon
55   cycle to climate change.

Current understanding of the factors that drive changes in τ are unclear due to the confounding effects of temperature and
moisture even though it is well perceived that temperature and water availability are the main climate factors that affect root
respiration and microbial decomposition (Raich, J. and W. H. Schlesinger,1992; Davidson and Janssens, 2006; Jackson, R.
B., et al., 2017). Therefore, it is difficult to implement local temperature sensitivity of τ into carbon cycle models due the
60   large discrepancy between intrinsic and apparent sensitivity of τ to temperature. As the soil environment and climate are
highly heterogeneous in space, the temperature sensitivity of τ is substantially affected by other factors as spatial scale
decreases (Jung et al., 2017).

Model simulations and observations do not agree in how the global distribution of τ is related to climate. Carvalhais et al.

(2014) combined observational datasets that cover both low latitudes and circumpolar regions to estimate global τ and

65   compared with CMIP5 simulations. They found a divergent result of global simulated total terrestrial carbon stocks that range from 1101 Pg C to 3374 Pg C (mean difference of 36%) leading to a wide range of turnover times from 8.5 to 22.7 years (mean difference of 29%). The models also exhibit a large discrepancy in the τ-temperature and τ-precipitation relationships across different latitudes compared to observations. Koven et al. (2017) illustrated a higher sensitivity of τ to temperature in cold regions than in warm regions using an observational-based soil dataset. They found that most of the

70   ESMs fail to capture the global τ – temperature pattern. The difficulty of evaluating the response of soil carbon to climate change is partly due to the fact that the dynamical observations at relevant timescales e.g. multi-decadal to centennial are lacking and the magnitude of projected change of τ to climate change is still poorly constrained (Koven et al., 2017).

There are not only large differences between simulations and observation-based estimates of τ, studies also show differences in the current observation-based estimates themselves. Specifically, estimates of global total carbon stock are characterized

75   by large uncertainties as different in-situ measurements and methods were used to derive total carbon stocks (Batjes, 2016; Hengl et al., 2017; Sanderman et al., 2017). Alongside recent soil carbon datasets (Tifafi et al., 2018), there are also several different global vegetation biomass (Thurner et al., 2014; Avitabile et al., 2016; Saatchi et al., 2017; Santoro et al., 2018) and GPP (Gross Primary Production) (Jung et al., 2017) products which may lead to substantial differences in the global τ distribution and its relationship with climate. Thus, there is an urgent need to construct an ensemble of global τ estimates

80   derived from different products and to quantify the uncertainty of the τ response to climate.

This study thus aims at developing an ensemble global estimation of τ which is derived from different observation-based products. Specifically, we will (1) update τ estimations with multiple state-of-the-art datasets; (2) quantify the contribution of the different components of τ to the global and local uncertainties; (3) identify the robust patterns across different ensemble members.

85   2 Datasets

The attributes of the τ dataset provided in this study, and the key external datasets that were used to estimate τ are summarized in Table 1. Details for each dataset are described in the below subsections.

2.1 Soil organic carbon datasets

Estimation of global soil carbon stock (C_{soil}) was based on five datasets that are derived from different approaches of

90   estimating soil carbon:

   a.   SoilGrids is an automated soil mapping system that provides consistent spatial predictions of soil properties and types in the original spatial resolution of 250m (Hengl et al., 2017). Global compilation of soil profiles is used to produce automated soil mapping based on machine learning algorithms. The data contains global soil organic carbon content at intervals of 0, 5, 15, 30, 60, 100 and 200 cm. In addition, chemical and physical properties such as bulk density and

95   carbon concentration are provided. 158 remote-sensing based covariates including land cover classes, long-term averaged surface temperature was used to fit the model. According to Hengl et al. (2017), the new version of the dataset can explain more of the variance (68.8%) in soil carbon stock than the previous version (22.9%) (Hengl et al., 2014). However, it has also been recognized that the current version of SoilGrids (released on 2017.08.01, ftp://ftp.soilgrids.org/data/recent) may overestimate carbon stocks due to high values of bulk density (Tifafi et al., 2018).

100   In general, the estimation of C_{soil} is hampered by the available measurements, especially in the circumpolar regions. Even though in-situ measurements had a large spatial extent and cover most of the continents, the regions that are characterized by severe climate or remoteness were much less sampled.

b.   The dataset of soil carbon provided by Sanderman et al. (2017, hereafter S2017) used the same method as SoilGrids but different input covariates. The main difference between SoilGrids and S2017 is that in addition to topographic,

105   lithological, climatic covariates, S2017 also incorporated land use and forest fraction into the model fitting. The relative importance analysis based on Random Forest model shows that soil depth, temperature, elevation and topography are the most important predictors which is similar to the model fitting results of SoilGrids. Land use types such as grazing and cropping land area also contributes significantly to the variance. The dataset provides soil carbon stocks at soil depths of 0-30 cm, 30-100 cm and 100-200 cm and at a spatial resolution of 10 km.

110   c.   Harmonized World Soil Database (HWSD) was also used in this study which utilized over 16000 standardized soil-mapping units worldwide which are harmonized into a global soil dataset (Batjes et al., 2016). HWSD is a 30 arc-second raster database that provides soil properties including organic carbon, PH, water storage capacity, soil depth at topsoil (0-30 cm) and subsoil (30-100 cm). HWSD combined regionally and nationally updated soil information worldwide to estimate soil properties in a harmonized way, and yet reliability of the data varies due to the different data sources. The

115   database which was derived from the Soil and Terrain (SOFTER) database had the highest reliability (Central and Eastern Europe, the Caribbean, Latin America, Southern and Eastern Africa) while the database that derived from the Soil Map of the World (North America, Australia, West Africa and Southern Asia) has a relatively lower reliability.

d.   We used the Northern Circumpolar Soil Carbon Database (NCSCD), which quantified soil organic carbon storage specifically in the northern circumpolar permafrost area (Hugelius et al., 2013). The dataset contained northern

120   circumpolar soil organic carbon content for depths of 0-30, 0-100, 100-200, 200-300 cm. The soil samplings included pedons from published literature, existing datasets and unpublished material. The 200 and 300 cm depth soil data was obtained by extrapolating the lowermost available values for bulk density and carbon content for a specific pedon to the full depth if the field data were only available in the first 50 cm of the full soil depth. However, the deep soil carbon (100-300 cm) showed the lowest level of confidence due to lack of in-situ measurements and much lower spatial

125   representativeness. The data was downloaded from https://bolin.su.se/data/ncscd/.

e.   The soil carbon stock and properties produced by the LandGIS maps development team (hereafter LandGIS) were also used in this study (Wheeler and Hengl, 2018). The soil profiles that were used in the training had a wide geographic coverage of America, Europe, Africa and Asia. One unique feature of LandGIS is that it included the soil profiles of Russia from the Dokuchaev Soil Science Institute/Ministry of Agriculture of Russia, which significantly improved the

130   predictions of C_{soil} in Russia. Different machine learning methods including random forest, gradient boosting and multinomial logistic regression were used to upscale the soil profiles to a global gridded dataset. Continuous 3D soil properties were predicted at 6 standard depths: 0, 10, 30, 60, 100 and 200cm. In comparison with the SoilGrids dataset, LandGIS added new remote sensing layers as covariates in the training and used 5 times more training points (360000 soil profiles) than SoilGrids (70000 soil profiles). The data was downloaded from

135   https://zenodo.org/record/2536040#.XYs1wpP7TUI.

2.2 Vegetation biomass datasets

Four different datasets of biomass at global scale were used to produce the total vegetation biomass (C_{veg}).

a.   Thurner et al. (2014) estimated the above-ground biomass (AGB) and below-ground biomass (BGB) for northern

140   hemisphere boreal and temperate forests (0.01° resolution, representative for the year 2010) based on satellite radar remote sensing retrievals of growing stock volume (GSV) and field measurements of wood density and biomass allometry. The carbon stocks of tree stems were estimated based on GSV retrieved with the BIOMASAR algorithm using remote sensing observations from the ASAR instrument on Envisat Satellite (Santoro et al., 2015), which was then converted to biomass using wood density information. The other tree biomass compartments (BC) including roots,

145   foliage and branches were estimated from stem biomass based on field measurements of biomass allometry. The total carbon content of the vegetation was derived as the sum of the biomass of the different compartments, which was then converted to carbon units using carbon fraction parameters. Comparison between the biomass map and inventory-based data shows good agreement at regional scales in Russia, the United States and Europe (Thurner et al., 2014). Since data from Thurner et al only covered northern boreal and temperate forests (30-80°N), we used data from Saatchi et al (2011)

150   to cover the lower latitudes.

b.   We also incorporated a map of forest biomass carbon stocks for the tropical regions provided by Saatchi et al., (2011). The map was derived using lidar, optical and microwave satellite imagery, trained using 4079 in-situ forest inventory plots (Saatchi et al., 2011). The method used GLAS Lidar observations to sample forest structure and used a power-law functional relationship to estimate biomass from the Lidar-derived Lorey's height of the canopy. This extended sample

155   of biomass density is then extrapolated over the landscape using MODIS and radar imagery, resulting in a pantropical AGB map. BGB was estimated as a function of AGB and the two were used together to derive total forest carbon stock at a 1 km spatial resolution.

c.   The GlobBiomass map (Santoro et al., 2018) estimateed GSV and AGB density at global scale for the year 2010 at 100 m spatial resolution. The AGB was derived from GSV using spatially explicit Biomass Expansion and Conversion

160   Factors (BCEF) obtained from an extensive dataset of wood density and compartment biomass measurements. GSV was estimated using space-borne SAR imagery (ALOS PALSAR and Envisat ASAR), Landsat-7, ICESAT LiDAR and auxiliary datasets, using the BIOMASAR algorithm to relate SAR backscattered intensity with GSV (Santoro et al., 2018b)

d. A pantropical AGB map (Avitabile et al., 2016) that combined two existing AGB datasets (Saatchi et al., 2011; Baccini
165 et al., 2012) was also incorporated in the data ensemble. This map used a large independent reference biomass dataset to
calibrate and optimally combine the two maps. The fusion approach was based on the bias removal and weighted-
average of the input maps (Ge et al., 2014), which incorporated the spatial patterns presented by the reference data in the
fused map. The resulting map presents a total AGB stock for the tropics which was 9-18% lower than the two input
maps and gave different spatial patterns over large areas. The fused biomass map has a spatial resolution of 1 km.
170

2.3 Soil depth dataset

A soil depth dataset was obtained from the Global Soil Texture and Derived Water-Holding Capacities database (Webb, et
al., 2000). Standardized values of soil depth and texture on a global scale, which were selected for the same soil types for
each continent, were contained in the database.

175 ## 2.4 The FLUXCOM global gross primary productivity dataset

FLUXCOM is an initiative to upscale biosphere-atmosphere fluxes measurements from eddy covariance flux towers
(FLUXNET) to global scale (Jung et al., 2017). We used the annual means of GPP using estimates from different machine
learning methods and two flux partitioning methods trained on daily carbon fluxes (Tramontana et al., 2016). In order to
produce high resolution (0.083º) spatial grids of carbon fluxes, only high-resolution satellite-based predictors were used in
180 model training. In this study, we derived the long-term mean annual GPP by averaging annual GPP from 2001 to 2014.

2.5 Climate datasets

A high spatial resolution (~1km) climate dataset WorldClim 2 (Fick and Hijmans, 2017) was used to investigate the
relationship between τ and climate. The data included monthly maximum, minimum and average temperature, precipitation,
solar radiation, vapor pressure and wind speed. The data was produced by assimilating between 9000 to 60000 ground-
185 station measurements and covariates such as topography, distance to the coast, and remote-sensing satellite products
including maximum and minimum land surface temperature, and cloud cover in model fitting. For different regions and
climate variables, different combinations of covariates were used. The two-fold cross-validation statistics showed a very
high model accuracy for temperature-related variables (R > 0.99), and a moderately high accuracy for precipitation (r =
0.86).

190 Table 1. Summary of the τ database and external datasets attributes.

Dataset source	Dataset name	Horizontal coverage	Horizontal resolution	Vertical resolution	File format	External link
				C_{soil}		
Sanderman et	S2017	Global	10km	0,30,100,200	GeoTIFF	https://github.com/whrc/Soil-Carbon-

				cm		Debt/tree/master/SOCS
SoilGrids	SoilGrids	Global	250m	0,5,15,30,60, 100,200cm	GeoTIFF	https://files.isric.org/soilgrids/data/
LandGIS	LandGIS	Global	250m	0,10,30,60,1 00,200cm	GeoTIFF	https://zenodo.org/record/2536040#.XhxHRBf0 kUF
Harmonized World Soil Database	HWSD	Global	1km	0,30,100cm	Raster	http://www.fao.org/soils-portal/soil-survey/soil-maps-and-databases/harmonized-world-soil-database-v12/en/
The Northern Circumpolar Soil Carbon Database	NCSCD	Circumpolar	1km	0,30,60,100, 200,300	GeoTIFF/ NetCDF	https://bolin.su.se/data/ncscd/
WoSIS Soil Profile Database	WoSIS	Global	In-situ	0-300cm	Shape	https://www.isric.org/explore/wosis/accessing-wosis-derived-datasets
International Soil Carbon Network	ISCN	Global	In-situ	0-400cm	Microsoft Excel	https://iscn.fluxdata.org/
Global Soil Texture And Derived Water-Holding Capacities database	Full soil depth	Global	100km	Single layer	ASCII	https://daac.ornl.gov/SOILS/guides/Webb.html
				C_{veg}		
Global biomass dataset	Saatchi	Global	1km	Single layer	GeoTIFF	Dataset available from provider (Saatchi et al., 2011)
GEOCARBON global forest biomass	Avitabile	Global	1km	Single layer	GeoTIFF	http://lucid.wur.nl/datasets/high-carbon-ecosystems
Integrated global biomass dataset	Saatchi-Thurner	Global	1km	Single layer	GeoTIFF	https://www.pnas.org/content/108/24/9899 https://onlinelibrary.wiley.com/doi/full/10.1111 /geb.12125
GlobBiomass	Santoro	Global	1km	Single layer	GeoTIFF	https://globbiomass.org/
				GPP		
FLUXCOM	GPP	Global	10km	Single layer	NetCDF	http://www.fluxcom.org/

Earth System
Science
Data

Open Access
Discussions

				Climate		
WorldClim	Mean annual temperature Mean annual precipitation	Global	1km	Single layer	GeoTIFF	http://worldclim.org/version2
				τ database		
τ database	Terrestrial carbon turnover times	Global	50km	100, 200, FD (cm)	NetCDF	https://www.bgc-jena.mpg.de/geodb/projects/FileDetails.php

3 Methods

3.1 Estimation of ecosystem turnover times

The total land carbon storage can be estimated by summing soil carbon stocks derived from extrapolation and vegetation
biomass. Assuming steady state in which the total efflux (autotrophic and heterotrophic respiration, fire, etc.) equals to influx
(GPP). Then τ can be calculated as the ratio between carbon stock and influx:

$$\tau = \frac{C_{soil} + C_{veg}}{GPP}$$

Here C_{soil} and C_{veg} are the total soil and vegetation carbon stocks, respectively.

3.2 Estimation of global vegetation biomass stock

The aboveground biomass datasets only contain biomass of trees, meaning the herbaceous part is not considered. To account
for herbaceous biomass, we used the same method as Carvarhais et al. (2014) which assumed the live vegetation fraction has
a mean turnover time of one year, then using a uniformly distributed probability distribution of respiratory costs between 25
to 75 percent, we were able to relate GPP with the carbon stock of vegetation as:

$$C_H = GPP \cdot (1 - \alpha) \cdot f_H$$

Where C_H is the carbon stock for the herbaceous vegetation biomass; GPP is based on the FLUXCOM estimations; α is the
percentage of respiration cost and f_H is the fraction of herbaceous part for each grid cell based on the SYNMAP database
(Jung et al., 2006).

Two vegetation biomass datasets (GlobBiomass and the Avitabile dataset) do not include BGB, in contrast to Saatchi's and
Thurner's products. In order to make all C_{veg} products comparable, we estimated the BGB from the empirical relationship
bewteen AGB and BGB derived previously by Saatchi et al. (2011):

8

$$BGB = 0.489 \cdot AGB^{0.89}$$

3.3 Extrapolation of soil datasets

Extrapolation is necessary to obtain the accumulated carbon stock from surface to full soil depth because the soil datasets only extend to 2 meters below the surface. However, a large amount of C_{soil} is stored below this depth, especially in peatland where soil carbon content is much higher in deeper soil (Hugelius et al., 2013). To estimate the total carbon storage in the land ecosystem, different empirical mathematical models were used (Table S1). The Covariance Matrix Adaptation Evolution Strategy (CMA-ES) method was used to optimize parameters of the models. The CMA-ES method is based on an evolutionary algorithm which used the pool of stochastically generated parameters of a model as the parents for the next generation.

Extrapolation, which involves using empirical numerical models, may cause arbitrary bias and higher uncertainty if the models are not appropriately chosen. Here we used the in-situ observational data from the World Soil Information Service (WOSIS) (Batjes et al., 2019) and the International Soil Carbon Network (ISCN) (Nave et al., 2017) to select the ensemble of the models that could best simulate soil carbon stocks at full depth. The approach (i) fit of each empirical model against cumulative C_{soil} with all data points up to 2m; then (ii) predicted the cumulative C_{soil} at full depth for each soil profile independently. The ability of a particular empirical model or combination of models (see Section 3.2) was then evaluated by comparing the predictions of C_{soil} at full depth against the observations. This procedure was applied on the two different in situ datasets, WOSIS which covers most of the biomes and ISCN which has more coverage in circumpolar regions. Finally, after comparing different model averaging methods (see supplement Table S2) we chose two model ensembles that could best represent circumpolar and non-circumpolar regions based on observational datasets, respectively. The performance of the chosen ensembles is synthesized in Figure S3 and S4.

3.4 Uncertainty analysis

We performed a N-way ANOVA on different variables in order to calculate the uncertainties that stem from different data sources. The method can provide the sum of square variance and the total variance which derived the contribution of each data source to the total uncertainty. We defined the final contribution from each component involved in the calculation of τ as

$$C_n = \frac{SS_n}{SS_{total}}$$

Where C_n is the contribution of uncertainty from a certain variable SS_n, SS_{total} is the sum of square variance of all variables. The contributions of uncertainties from soil, vegetation, GPP and soil depth of all ensemble members to the target variable τ were calculated. The uncertainty analysis reflects the relative spread of each group and the effect on the spread of τ.

3.5 The analysis of zonal correlations

The local correlation between τ and climate across latitudes was obtained by using a zonal moving window approach in which the Pearson partial correlations between τ and MAT/MAP were calculated using a 360º (longitudinal span) ×2.5º (latitudinal span) moving window. This approach allowed for the assessment of the relative importance for each climate
250 parameter. The lowest and highest 1% of data points in each moving window was removed to avoid the effect of potential outliers. In order to investigate the effect of latitudinal span, we chose different band size of 0.5º, 2.5º and 5º and performed the correlation analysis in the same manner for each selection.

4 Results

255 ### 4.1 The global carbon stock

Table 2 shows the estimates of C_{soil} and GPP. Globally, estimates of soil carbon stocks within the top 2-meters of soil are 2749 PgC, 3628 PgC and 3546 PgC for the datasets of S2017, SoilGrids and LandGIS, respectively (bulk density corrected, see Supplement). The significant differences among different datasets indicate a high uncertainty in our current estimation of global soil carbon storage. The extrapolation of C_{soil} to full soil depth (FD) shows that approximately 18% of carbon stored is
260 below 2 meters. Compared to the previous generation of soil data HWSD (available only within the top 1 meter), the state-of-the-art datasets of the current study have significantly higher carbon stocks within the top 1-meter of soil (Table 2). On the other hand, the current datasets of vegetation biomass shows global C_{veg} ranges from 407 to 451 PgC and has less relative uncertainty. The estimation of GPP shows a narrow range of 99 to 106 PgC from different products. Overall, the results show the difference in C_{soil} is much larger than C_{veg} and GPP.

265

Table 2. Estimates of soil organic carbon stocks, vegetation biomass and GPP (Pg C).

Carbon stock in PgC	Non-circumpolar			Circumpolar			Global		
C_{soil}	0-1m	0-2m	0-FD	0-1m	0-2m	0-FD	0-1m	0-2m	0-FD
S2017	1215	1861	2131	510	887	1020	1725	2749	3152
SoilGrids	1399	2292	2944	796	1335	1326	2195	3628	4269
LandGIS	1305	2093	2606	787	1453	1766	2091	3546	4372
HWSD	764	N/a	N/a	568	N/a	N/a	1332	N/a	N/a
NCSCD	N/a	N/a	N/a	567	868	N/a	N/a	N/a	N/a
Mean	1171	2082	2560	646	1136	1371	1836	3308	3931
Median	1260	2093	2606	568	1111	1326	1908	3546	4269
C_{veg}									
Saatchi	358			49			407		
Avitabile	412			39			451		
Saatchi-Thurner	399			38			437		

Santoro	393	42	435
Mean	391	42	433
Median	396	41	436
GPP			
Mean	96	7	102
Median	96	6	102
P10	92	6	99
P90	99	8	106

4.2 The regional soil organic carbon stocks

A significant amount of soil organic carbon is stored in high-latitude terrestrial ecosystems, especially in the permafrost
270 region (Hugelius et al., 2013). However, in comparison with low latitudes, the uncertainties of C_{soil} distribution and storage
in high latitudes are potentially higher due to fewer available observations of soil profiles. We therefore divided the global
soil carbon into the non-circumpolar (Figure 1) and the circumpolar (Figure 2) regions based on the northern permafrost
region map of NCSCD. The results show that the mean value and range (maximum - minimum) of C_{soil} in non-circumpolar
region (Table 2) in the top 2m is 2082 PgC and 431 PgC (20% of mean value) and that in the circumpolar region within the
275 top 2m is 1225 PgC and 566 PgC (46% of mean). The extrapolation of C_{soil} to full soil depth in non-circumpolar region led
to a higher mean value of 2560 PgC and range of 813 PgC (32% of mean) and 1371 PgC and 746 PgC (54% of mean) in the
circumpolar region. The results show that the relative difference of C_{soil} in circumpolar regions is two times larger than that
in non-circumpolar regions among all datasets.

4.3 The spatial distribution of soil carbon stock

280 The spatial distribution of C_{soil} is more consistent across datasets in the non-circumpolar region than in the circumpolar
region (Figure 1). The correlation coefficients (r) between each pair of datasets in the non-circumpolar region are generally
higher than in the circumpolar region. Our results show a moderate agreement among the datasets in the spatial distribution
of C_{soil} globally (r>0.65). However, there are significant differences in the spatial patterns between the HWSD and each of
the recent datasets (Figure 1) as the correlation coefficients are all below 0.3. In addition, there is 2-fold lower carbon
285 storage in the HWSD than the other datasets. Ratios between the total C_{soil} in the top 100 cm (Fig 1: upper off diagonal plots)
show that LandGIS, SoilGrids and S2017 are consistent in temperate regions but show poor agreement in the tropical and the
boreal regions. The comparison also shows that the gradient in carbon stocks between Europe and the lower latitudes
diminished in the HWSD soil map. In addition, the spatial distribution and the amount of carbon stocks in Indonesia is
significantly different in the HWSD.

290 Higher dissimilarities of spatial patterns across the datasets in the circumpolar region is shown in Figure 2. We included the
NCSCD dataset, which specifically focuses on the circumpolar region. The spatial correlations between each pair of the four
datasets show low r values, which range from 0.2 to 0.5. In contrast with the non-circumpolar region, the high spatial

dissimilarity in circumpolar region indicates higher uncertainty regarding the estimation of total carbon storage. However, there is no clear evidence on which dataset is more credible in terms of total carbon storage and spatial pattern. The large

295 differences are possibly due to fewer observational soil profiles in the northern high-latitude regions, which are crucial is the model training process.

4.4 The vertical distribution of global carbon stock

The comparison of all datasets shows that there is a good agreement in the vertical structure of terrestrial carbon stocks. The

300 C_{soil} in the top 1-meter is about half of the total terrestrial carbon and 80% for the top 2-meter C_{soil} regardless of region or data source. For the non-circumpolar region, all the datasets show significantly higher carbon storage in the top 1m (451-635 PgC higher) than that in the HWSD, while showing less divergence of carbon storage among these three datasets (Table 2). In general, the current datasets show similar vertical distribution of C_{soil} with consistent values and ratios between 1m and 2m soil. The extrapolation results indicate that about 15% of carbon is stored below 2m in the non-circumpolar region. For

305 the circumpolar region, the four datasets show a clear trend that the difference of C_{soil} increases with soil depth, as shown in Table 2. The difference between the top 1m C_{soil} among datasets has a higher difference than that of 2m. However, the ratio between storage in 1m and 2m is similar across all datasets.

4.5 The ecosystem carbon turnover times and associated uncertainties

Using C_{soil}, C_{veg} and GPP, we estimated the carbon turnover times with different combinations of datasets in order to

310 quantify the uncertainty. We calculated τ in the same manner as the previous study (Carvalhais et al., 2014) in which they used only 1m of soil in the circumpolar region and full soil depth in the non-circumpolar region. Our estimation of global mean τ is 35 years with an interquartile range of 31 to 44 years, which is much higher than the previous study of 23 years (interquartile range: 19 to 30 years). In addition, we derived a global τ of 42 years with an interquartile range of 37 to 51 years by assuming the maximum active layer thickness to be the full soil depth in the circumpolar regions instead of using

315 only 1-meter C_{soil} as was done in the previous study. The incorporation of deep soil in the circumpolar region increased the global τ by 7 years. The global spatial distribution of τ (Figure 3) shows great heterogeneity, which ranges from 5 years in the tropics to over 1000 years in northern high latitudes. The results show a U-shaped distribution of τ along latitudes where τ increases nearly three orders of magnitude from low to high latitudes. Figure 3b shows the map of relative uncertainty that is derived from different datasets. The higher relative uncertainty indicates more spread among the datasets used to estimate

320 τ. Our result shows that peatland and arid regions generally have higher uncertainties than the rest of the world. We found several regions with very different estimations of τ among the datasets including north-east Canada, central Russia and central Australia where the relative uncertainties are over 100%.

C_{soil}, C_{veg} and GPP contribute differently to the overall uncertainty of τ as shown in Figure 4. The difference among soil datasets is the dominating factor of τ uncertainty, especially in the circumpolar regions and the Indonesian peatland where

325 there is large amount of soil organic carbon in subsoil. On the other hand, the uncertainties of τ in arid and semi-arid regions

are controlled by the difference in GPP products. The contribution of vegetation to the uncertainty in τ is most significant in the tropics and warm temperate regions where there is large vegetation biomass. It is worth to note that contributions from each component also vary with depth of carbon stock that was used to calculate τ. For instance, the uncertainty contribution from C_{veg} becomes smaller when the C_{soil} up to 2 meters is used compared to only using 1-meter in calculating τ. However,

330 the fact that the difference in the soil products was the major contributor to the τ uncertainty remains no matter what soil depth is used. Overall, the uncertainty of τ is mostly derived from soil and GPP, which dominate 68% and 22% of the global land area, while vegetation plays a minor role globally (3%).

4.6 The zonal pattern of turnover times

The latitudinal distributions of τ can be best represented by a second-degree polynomial function (Figure 5b). After fitting

335 the data of all ensemble members, the rate of τ change with latitude can be obtained by taking the first derivative of the fitted polynomial function. We found that the rate of τ change (Figure 5c) has very consistent zonal patterns for different τ ensemble members from different data sources. The result shows a consensus on the change of τ with latitude of different datasets. We also found that the zonal τ gradients were not significantly (P > 0.05) different from each other for different selections of soil depth, indicating soil depth has no significant effect on the τ gradient along latitude. It is worth to note that

340 there is a significant difference in the zonal τ gradient between the northern and southern hemisphere (P < 0.0001) and that τ increases faster from low to high latitude in northern latitudes than in the southern latitudes. The results show that we have high confidence in the zonal distribution of τ and that the difference across datasets does not affect the robustness of the pattern.

4.7 The zonal correlation between turnover time and climate

345 The correlations between τ and mean annual temperature and mean annual precipitation are analysed for all the ensemble members on global scale (see Method section). The correlation (Figure 6a) is the strongest in northern mid-to-high latitudes between 25º N and 60 º N, and it decreases rapidly from 20º N to the equator. In the southern hemisphere, it increases until 40º S, albeit having a weaker gradient than in the northern hemisphere. The uncertainties originating from different data sources are shown by the shaded area (Figure 6a and 7d). The result shows that there are high uncertainties in the transitional

350 regions between the temperate and Arctic regions (50 – 70º N) as well as tropical regions (20º N to 20º S). Similar to the previous result of uncertainty contribution where soil is the dominating factor, the differences in C_{soil} also cause the spread in τ - T correlation. However, the patterns of correlation along latitude do not change regardless of the data source and the soil depth. All ensemble members agree that τ is negatively associated with temperature, with stronger associations in cold regions than in warm regions.

355 The correlation between τ and precipitation, in general, has larger variability across latitude and a higher uncertainty due to differences in data (Figure 6b). Contrary to the τ - T relationship, the uncertainty of the τ - P relationship derived from both different data sources and soil depths are smaller in the tropics than in high latitudes. Negative correlations dominate the latitudes between 20 and 50º N as well as between 20 and 40º S, while there is a stronger positive correlation in the tropics.

360   There is a shift in the sign of the correlation coefficient from negative in temperate zone to positive in tropics, indicating the role of water changes from water-limited regions to water-excessive regions.

5 Discussion

In this section, we will discuss the robustness of the current state-of-the-art estimation on global terrestrial carbon turnover times and their response to climate change. We first show the variation of spatial and vertical distribution of carbon stock in different regions and the possible reason for the difference, and we then discuss the robustness of zonal distribution of

365   turnover times and zonal changing rates across different datasets. Finally, we focus on the sensitivity of turnover times to climate and implications.

5.1 Estimation of global carbon stock

Accurate estimation of terrestrial carbon storage and turnover time are essential for understanding carbon cycle-climate feedback. Our analysis benchmarks soil carbon storage from multiple state-of-the-art observational based datasets at global

370   scale and provide not only an estimate of the total stock of soil carbon but also the vertical distribution and spatial variability of soil carbon storage. We divide the global map into circumpolar and non-circumpolar regions due to the different characteristics and uncertainty.

We found that there is a significant difference across the current soil carbon datasets in both circumpolar and non-circumpolar regions. The results show that the uncertainty of C_{soil} estimations in the circumpolar region is two times larger

375   than that of the non-circumpolar region. The spatial patterns of total ecosystem C_{soil} among the soil datasets are more consistent in the non-circumpolar region than in the circumpolar region. In contrast with the non-circumpolar region, there is lower confidence in the circumpolar region in estimating C_{soil} due the fact that there is low spatial correlation across datasets. The difference can be caused various reasons. As an important input to the machine learning method, in-situ soil profiles are very important factors that influence the final results of the upscaling. The sparse coverage of soil profiles in the

380   circumpolar region may cause the large divergence in the northern circumpolar region. A major difference between S2017 and the other two soil datasets is that soil carbon stock was a direct target of upscaling in the former dataset, while in the latter two datasets each component used to calculate C_{soil} (carbon density, bulk density and percentage of coarse fragments) was predicted individually. In addition, the climatic covariates that were used in the upscaling were different (see Method).

In contrast with the non-circumpolar region, the circumpolar C_{soil} does not have a decreasing trend up to 4 meters of soil

385   depth (Figure S1) which indicates that there is a significant amount of carbon stores in deep soil. The deep soil turnover is a key process to the global carbon cycle yet poorly understood. In this study, we extrapolated the soil carbon stock to full soil depth. We chose the model ensembles from a framework to pick out the models that had a minimum distance between prediction and observations by using in-situ soil profiles (see Supplement). Two model ensembles were selected that can best represent the soil vertical distribution in circumpolar and non-circumpolar regions. The final results depend on the

390   information from the soil profiles and also the characteristics of the empirical models. The extrapolation gave us insights to

the carbon storage and vertical distribution in deep soil. The results of extrapolation show there is approximately 15% of carbon stored below 2 meters globally and over 20% of carbon stored below 2 meters in the northern circumpolar region. Although the total amount of carbon storage in the ecosystem shows a large divergence among different datasets, the ratio between different soil depths are quite consistent indicating a high confidence in the vertical structure of soil compare

395 to the total amount.

The global soil carbon stocks across observational-based datasets are much less divergent than the current earth system model (ESM) simulations. The CMIP5 results show the simulated carbon storage ranges from 500-3000 PgC making τ varies by a factor of 3.6, from 11 to 39 years (Todd-Brown et al., 2013). Our results show that the amount of carbon in the ecosystem is much higher than the estimation by ESMs. Even the lowest estimation (S2017 dataset) of total carbon storage is

400 about 500 PgC higher than the highest ESM estimation (MPI-ESM-LR). The spatial distribution of carbon stocks among ESMs have a large variation across models while the observational-based datasets are more consistent in the non-circumpolar region. But we leave a question mark to the soil carbon in the circumpolar region, which is characterized by large uncertainty as shown by the current observational-based soil datasets.

5.2 The terrestrial carbon turnover time and uncertainty

405 The uncertainty analysis showed that our current estimation of τ has a considerable spread which derived from the state-of-the-art observations of soil, vegetation and carbon fluxes. In this study, we showed the uncertainty is contributed mainly by the soil carbon stock and GPP, where the former dominates the vast areas in the circumpolar region and the tropical peatland while the latter dominates the semi-arid and arid regions. However, the uncertainty comes not only from the differences across datasets but also from the soil depth we chose to estimate τ. The frozen permafrost soil in the circumpolar region,

410 although containing a large amount of carbon, remains inactive in the process of turnover. However, we do not know to what soil depth we should use in the τ estimation since currently our knowledge on the active layer thickness of frozen permafrost soil is still lacking. In addition, the active layer thickness of permafrost changes with climate, which adds more uncertainty to the estimation of τ. Thus, we argue that the current datasets cannot support robust estimation of global τ.

Although the current estimation of τ has a large variation, we show that the zonal distribution of τ is a robust feature that

415 changes little with different datasets, which indicates that the current state-of-the-art datasets all agree on the latitudinal gradient of the carbon turnover time. Another robust feature is that the zonal changing rate of τ does not change with the soil depth (Figure 5). It has always been a problem of what soil depth should we use to represent the functional part of carbon in the ecosystem. The selection of soil depth is usually arbitrary and varies from study to study. For example, Koven et al. (2017) and Wang et al. (2017) used the top one-meter of soil carbon to represent the total terrestrial carbon pool while

420 Carvalhais et al. (2014) extrapolated soil to full depth and used it as the pool. Our results demonstrate that the selection of the soil depth does not affect the zonal pattern that we observed. This can be better seen in the next section with the response of τ to climate.

5.3 Robust associations of τ and climate

The scope of this study is to find whether we can be certain about the response of τ to climate change on a long-term, broad-
425 scale with current τ estimations. It is well recognized that the sensitivity of terrestrial carbon to climate is a major uncertainty, which is reflected by the spread of τ estimation by the different ESMs. However, we need reliable estimations of τ to quantify the sensitivity and provide robust constraints to improve the performance of the current ESMs. We showed the zonal correlation between τ and temperature varies with latitude where high correlations are found in the high latitude and low to moderate correlation in low latitude, especially the tropics. The zonal pattern of τ-precipitation is more complicated in
430 that water availability can cause local variability to a great extent. The turnover times in the tropics is more sensitive to precipitation than to temperature as shown in Figure 6d. The role shifted along latitude between temperature and precipitation in the pattern of τ due to the variation in the relative importance for each parameter. However, the temperature gradient shaped the zonal distribution of τ as it can be seen that τ increases with latitude. All of these relationships are verified by each ensemble member of the data. We found the correlations, although they vary in strength, are very robust.
435 The intimate interaction of energy and water along with other factors such as land use change all affect τ but on different spatial and temporal scales. It is worth mentioning that the τ - T relationship is similar when compared with previous results (Carvalhais et al., 2014) whereas there are considerable differences in the τ - precipitation relationship, specifically in tropical regions where the turnover times were always negatively correlated with precipitation in previous study.

440 ## 6 Data availability

The dataset of whole ecosystem turnover times of carbon provided here can be downloaded
from: https://doi.org/10.17871/bgitau.201911 (Fan et al., 2019).

445 ## 7 Conclusion

A full assessment of the global turnover times of carbon is provided using an observational-based ensemble of current state-or-the-art datasets of soil carbon stocks, vegetation biomass and GPP. At the global scale, the uncertainties in τ estimates are dominated by the large uncertainties in soil carbon stocks. The uncertainty of carbon stocks and τ estimation in the circumpolar region is significantly higher than that in the non-circumpolar region. Our results show that there is a consistent
450 vertical distribution of soil carbon across datasets, and it is estimated that soils below 2 meters take up to 20% of total soil carbon globally. A spatial analysis shows that both soil carbon and GPP are the major contributors of local uncertainties in τ estimation. The differences in soil stocks between datasets dominates the uncertainties of τ in the circumpolar region and in tropical peatlands, while the spread in GPP dominates the uncertainty in semi-arid and arid regions. The difference in vegetation data has a minor contribution to the uncertainty.

455   Despite the differences, we identified several robust patterns that change only marginally across different ensemble members
       of τ that derived from different datasets or different soil depths. First, we found a consistent latitudinal pattern in τ that can
       be described by a second-degree polynomial function. The changing rate of τ with latitude can be described equally well for
       all ensemble members and the changing rate of τ with latitude is highly consistent across different datasets and does not
       change with soil depth. The same zonal correlations between τ and climate showed there is a robust association of τ with
460   temperature and with precipitation. However, we note that association between temperature/precipitation and τ change with
       latitude. Specifically, temperature mainly affects the τ variation in middle to high latitudes beyond 20ºN and 20ºS while
       precipitation affects τ not only in temperate zones but also in the tropical regions. Thus, the sensitivity of τ to a certain
       climate factor makes more sense to be calculated and interpreted in regions where the climate factor is the main driver of the
       τ variation. Overall, this study synthesizes the current state-of-the-art data on global carbon turnover estimation and argues
465   that the zonal distribution of τ and its response to climate is robust regardless of different datasets or assumptions on soil
       depth. This is a critical advancement since previous studies usually made arbitrary decisions on the soil depth that use to
       estimate τ, and supports exercises for benchmarking ESMs. Future studies should further investigate τ with regional spatial
       scale and its response to climate as well as other factors such as land use change, in order to have an in-depth understanding
       of carbon cycle turnover.

470

Author contributions

NF is the main author who wrote the manuscript. NC and MR supervised the analysis of the data and development of the
paper. SK intensively participate in the discussion and development of the paper. MT, VA, MS and BA provide feedbacks
on the scientific analysis and text of the paper. UW is technical support and responsible for data management.

475   **Competing interests**

The authors declare no conflict of interest.

References

Avitabile, V., Herold, M., Heuvelink, G., Lewis, S. L., Phillips, O. L., Asner, G. P., Armston, J., Ashton, P. S., Banin, L., and Bayol, N.: An integrated pan-tropical biomass map using multiple reference datasets, Global Change Biology, 22, 1406-1420, 10.1111/gcb.13139, https://onlinelibrary.wiley.com/doi/full/10.1111/gcb.13139, 2016.

485

Baccini, A., Goetz, S., Walker, W., Laporte, N., Sun, M., Sulla-Menashe, D., Hackler, J., Beck, P., Dubayah, R., and Friedl, M.: Estimated carbon dioxide emissions from tropical deforestation improved by carbon-density maps, Nature Climate Change, 2, 182, https://www.nature.com/articles/nclimate1354, 2012.

490 Barrett, D. J.: Steady state turnover time of carbon in the Australian terrestrial biosphere, Glob. Biogeochem. Cycle, 16, https://agupubs.onlinelibrary.wiley.com/doi/full/10.1029/2002GB001860, 2002.

Batjes, N.: Harmonized soil property values for broad-scale modelling (WISE30sec) with estimates of global soil carbon stocks, Geoderma, 269, 61-68, https://www.sciencedirect.com/science/article/pii/S0016706116300349, 2016.

495

Batjes, N. H., Ribeiro, E., and van Oostrum, A.: Standardised soil profile data to support global mapping and modelling (WoSIS snapshot 2019), Earth Syst. Sci. Data Discuss., https://doi.org/10.5194/essd-2019-164, in review, 2019.

Bolin, B., and Rodhe, H.: A note on the concepts of age distribution and transit time in natural reservoirs, Tellus, 25, 58-62, 500 https://onlinelibrary.wiley.com/doi/abs/10.1111/j.2153-3490.1973.tb01594.x, 1973.

Carvalhais, N., Forkel, M., Khomik, M., Bellarby, J., Jung, M., Migliavacca, M., Mu, M., Saatchi, S., Santoro, M., and Thurner, M.: Global covariation of carbon turnover times with climate in terrestrial ecosystems, Nature, 514, 213-217, https://www.nature.com/articles/nature13731, 2014.

505

Davidson, E. A., and Janssens, I. A.: Temperature sensitivity of soil carbon decomposition and feedbacks to climate change, Nature, 440, 165-173, https://www.nature.com/articles/nature04514, 2006.

Fan, N., Koirala, S., Reichstein, M., Thurner, M., Avitabile, V., Santoro, M., Ahrens, B., Weber, Ulrich., and Carvarhais, N.: 510 Ecosystem turnover time database, MPI-BGC, https://doi.org/10.17871/bgitau.201911, 2019

Friend, A. D., Lucht, W., Rademacher, T. T., Keribin, R., Betts, R., Cadule, P., Ciais, P., Clark, D. B., Dankers, R., and Falloon, P. D.: Carbon residence time dominates uncertainty in terrestrial vegetation responses to future climate and atmospheric CO2, Proceedings of the National Academy of Sciences, 111, 3280-3285, 515 https://www.pnas.org/content/111/9/3280, 2014.

Fick, S. E., and Hijmans, R. J.: WorldClim 2: new 1-km spatial resolution climate surfaces for global land areas, International Journal of Climatology, https://rmets.onlinelibrary.wiley.com/doi/full/10.1002/joc.5086, 2017.

520 Generation 3 Database Reports: Nave L, Johnson K, van Ingen C, Agarwal D, Humphrey M, Beekwilder N. 2017. International Soil Carbon Network (ISCN) Database, Version 3. DOI: 10.17040/ISCN/1305039. Database Report: ISCN_SOC-DATA_LAYER_1-1. Accessed 2 February 2019.

Klein Goldewijk, K., Beusen, A., Doelman, J., and Stehfest, E.: Anthropogenic land use estimates for the Holocene – HYDE 525 3.2, Earth Syst. Sci. Data, 9, 927–953, https://doi.org/10.5194/essd-9-927-2017, 2017.

Hengl, T., de Jesus, J. M., MacMillan, R. A., Batjes, N. H., Heuvelink, G. B., Ribeiro, E., Samuel-Rosa, A., Kempen, B., Leenaars, J. G., and Walsh, M. G.: SoilGrids1km—global soil information based on automated mapping, PloS one, 9, e105992, https://journals.plos.org/plosone/article?id=10.1371/journal.pone.0105992, 2014.

530

Hengl, T., de Jesus, J. M., Heuvelink, G. B., Gonzalez, M. R., Kilibarda, M., Blagotić, A., Shangguan, W., Wright, M. N., Geng, X., and Bauer-Marschallinger, B.: SoilGrids250m: Global gridded soil information based on machine learning, PloS one, 12, e0169748, https://journals.plos.org/plosone/article?id=10.1371/journal.pone.0169748, 2017.

535 Hugelius, G., Bockheim, J. G., Camill, P., Elberling, B., Grosse, G., Harden, J. W., Johnson, K., Jorgenson, T., Koven, C. D., Kuhry, P., Michaelson, G., Mishra, U., Palmtag, J., Ping, C.-L., O'Donnell, J., Schirrmeister, L., Schuur, E. A. G., Sheng, Y., Smith, L. C., Strauss, J., and Yu, Z.: A new data set for estimating organic carbon storage to 3 m depth in soils of the northern circumpolar permafrost region, Earth Syst. Sci. Data, 5, 393–402, https://doi.org/10.5194/essd-5-393-2013, 2013.

540 Wheeler, I., Hengl, T.: Soil organic carbon stock in kg/m2 time-series 2001–2015 based on the land cover changes (Version v0.2) [Data set]. Zenodo. http://doi.org/10.5281/zenodo.2529721, 2018

Jackson, R. B., Lajtha, K., Crow, S. E., Hugelius, G., Kramer, M. G., and Piñeiro, G.: The ecology of soil carbon: pools, vulnerabilities, and biotic and abiotic controls, Annual Review of Ecology, Evolution, and Systematics, 48, 419-445,
545 https://www.annualreviews.org/doi/abs/10.1146/annurev-ecolsys-112414-054234, 2017.

Jung, M., Reichstein, M., Schwalm, C. R., Huntingford, C., Sitch, S., Ahlström, A., Arneth, A., Camps-Valls, G., Ciais, P., and Friedlingstein, P.: Compensatory water effects link yearly global land CO2 sink changes to temperature, Nature, 541, 516-520, https://www.nature.com/articles/nature20780, 2017.
550
Koven, C. D., Hugelius, G., Lawrence, D. M., and Wieder, W. R.: Higher climatological temperature sensitivity of soil carbon in cold than warm climates, Nature Climate Change, 7, 817, https://www.nature.com/articles/nclimate3421, 2017.

Raich, J., and Schlesinger, W. H.: The global carbon dioxide flux in soil respiration and its relationship to vegetation and
555 climate, Tellus B, 44, 81-99, https://www.tandfonline.com/doi/abs/10.3402/tellusb.v44i2.15428, 1992.

Saatchi, S. S., Harris, N. L., Brown, S., Lefsky, M., Mitchard, E. T., Salas, W., Zutta, B. R., Buermann, W., Lewis, S. L., and Hagen, S.: Benchmark map of forest carbon stocks in tropical regions across three continents, Proceedings of the National Academy of Sciences, 108, 9899-9904, https://www.pnas.org/content/108/24/9899, 2011.
560
Sanderman, J., Hengl, T., and Fiske, G. J.: Soil carbon debt of 12,000 years of human land use, Proceedings of the National Academy of Sciences, 114, 9575-9580, https://www.pnas.org/content/114/36/9575, 2017.

Santoro, M., Beaudoin, A., Beer, C., Cartus, O., Fransson, J. E., Hall, R. J., Pathe, C., Schmullius, C., Schepaschenko, D.,
565 and Shvidenko, A.: Forest growing stock volume of the northern hemisphere: Spatially explicit estimates for 2010 derived from Envisat ASAR, Remote Sensing of Environment, 168, 316-334, https://www.sciencedirect.com/science/article/pii/S003442571530064X, 2015.

570 Santoro, M., Cartus, O., Mermoz, S., Bouvet, A., Le Toan, T., Carvalhais, N., Rozendaal, D., Herold, M., Avitabile, V., Quegan, S., Carreiras, J., Rauste, Y., Balzter, H., Schmullius, C., Seifert, F. M.: A detailed portrait of the forest aboveground biomass pool for the year 2010 obtained from multiple remote sensing observations, Geophysical Research Abstracts, vol. 20, pp. EGU2018-18932, EGU General Assembly, https://ui.adsabs.harvard.edu/abs/2018EGUGA..2018932S/abstract, 2018b.
575
Thurner, M., Beer, C., Santoro, M., Carvalhais, N., Wutzler, T., Schepaschenko, D., Shvidenko, A., Kompter, E., Ahrens, B., and Levick, S. R.: Carbon stock and density of northern boreal and temperate forests, Global Ecology and Biogeography, 23, 297-310, https://onlinelibrary.wiley.com/doi/full/10.1111/geb.12125, 2014.

580 Tifafi, M., Guenet, B., and Hatté, C.: Large differences in global and regional total soil carbon stock estimates based on SoilGrids, HWSD, and NCSCD: Intercomparison and evaluation based on field data from USA, England, Wales, and

France, Glob. Biogeochem. Cycle, 32, 42-56, https://agupubs.onlinelibrary.wiley.com/doi/full/10.1002/2017GB005678, 2018.

585 Todd-Brown, K., Randerson, J., Post, W., Hoffman, F., Tarnocai, C., Schuur, E., and Allison, S.: Causes of variation in soil carbon simulations from CMIP5 Earth system models and comparison with observations, Biogeosciences, 10, https://www.biogeosciences.net/10/1717/2013/bg-10-1717-2013.html, 2013.

Todd-Brown, K., Randerson, J., Hopkins, F., Arora, V., Hajima, T., Jones, C., Shevliakova, E., Tjiputra, J., Volodin, E., and
590 Wu, T.: Changes in soil organic carbon storage predicted by Earth system models during the 21st century, Biogeosciences, 11, 2341-2356, https://www.biogeosciences.net/11/2341/2014/, 2014.

Tramontana, G., Jung, M., Schwalm, C. R., Ichii, K., Camps-Valls, G., Ráduly, B., Reichstein, M., Arain, M. A., Cescatti, A., and Kiely, G.: Predicting carbon dioxide and energy fluxes across global FLUXNET sites with regression algorithms,
595 https://www.biogeosciences.net/13/4291/2016/, 2016.

Webb, R., C.E. Rosenzweig, and E.R. Levine.: Global Soil Texture and Derived Water-Holding Capacities. ORNL DAAC, Oak Ridge, Tennessee, USA. https://doi.org/10.3334/ORNLDAAC/548, 2000.

600 Wenzel, S., Cox, P. M., Eyring, V., and Friedlingstein, P.: Emergent constraints on climate-carbon cycle feedbacks in the CMIP5 Earth system models, Journal of Geophysical Research: Biogeosciences, 119, 794-807, https://agupubs.onlinelibrary.wiley.com/doi/full/10.1002/2013JG002591, 2014.

605
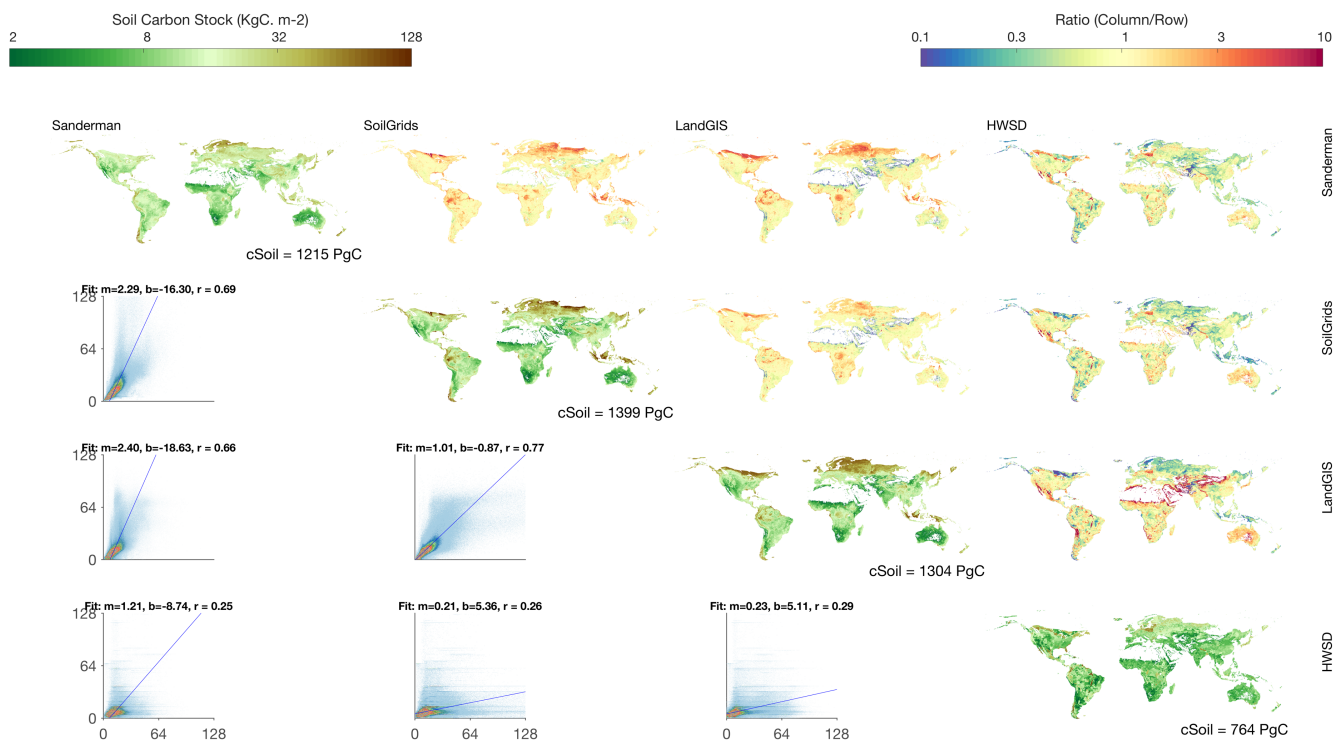
Figure 1: Spatial distribution of soil carbon storage at 0-100cm in non-circumpolar region. The total amount of carbon stock is shown in the bottom of each diagonal subplot. The upper off-diagonal are the ratios between each pair of datasets (column/row). The bottom off-diagonal subplots show the major axis regression between each pair of datasets (m: slope, b: intercept, r: correlation coefficient).
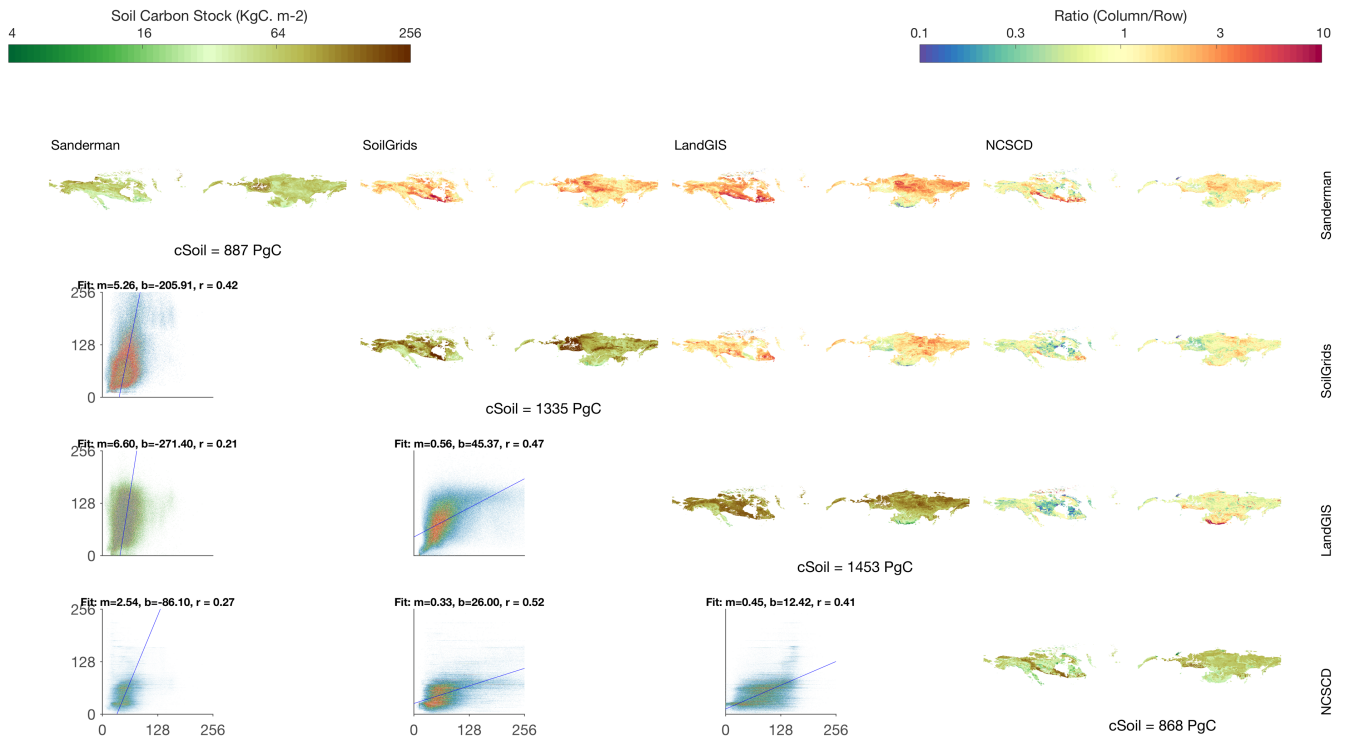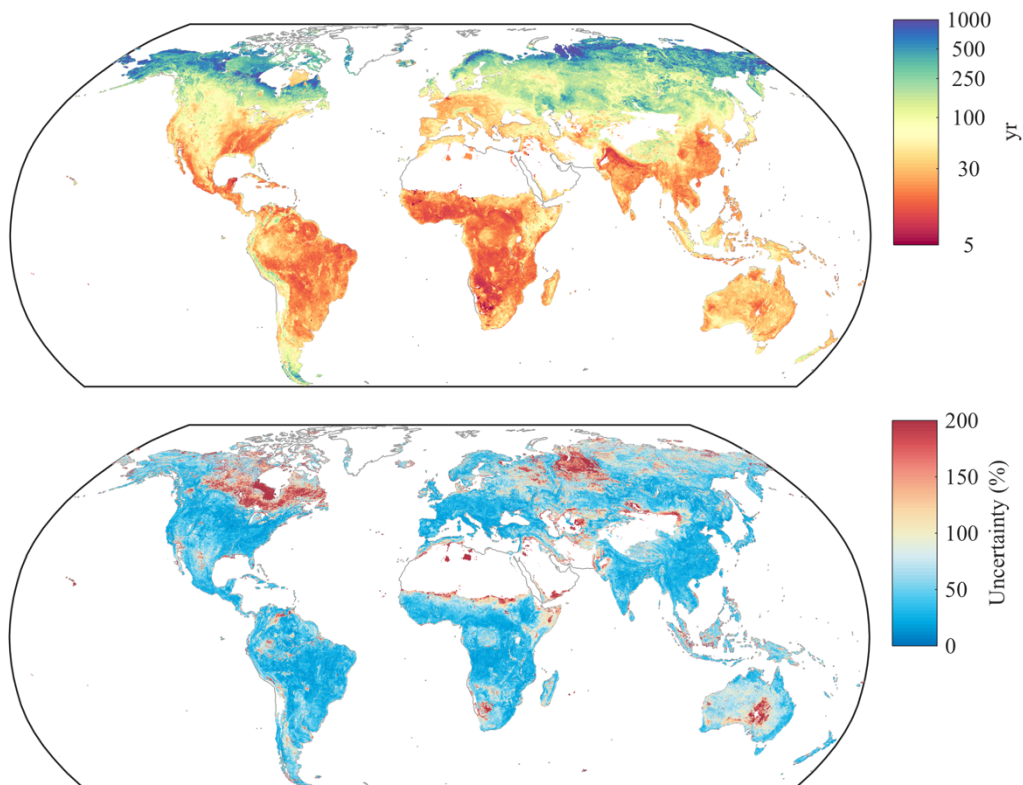
615

Figure 2: The same as Figure 1 except for the C_{soil} in 0-200cm in circumpolar region.

620

625

Figure 3: The spatial distribution of mean turnover time (in log scale) and relative uncertainty (Quantile range/mean). Upper subplot, spatial distribution of turnover times. Below subplot, relative uncertainty.
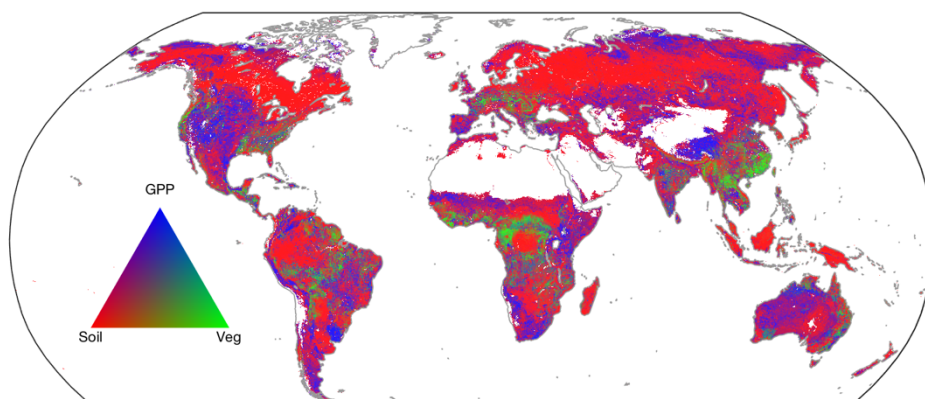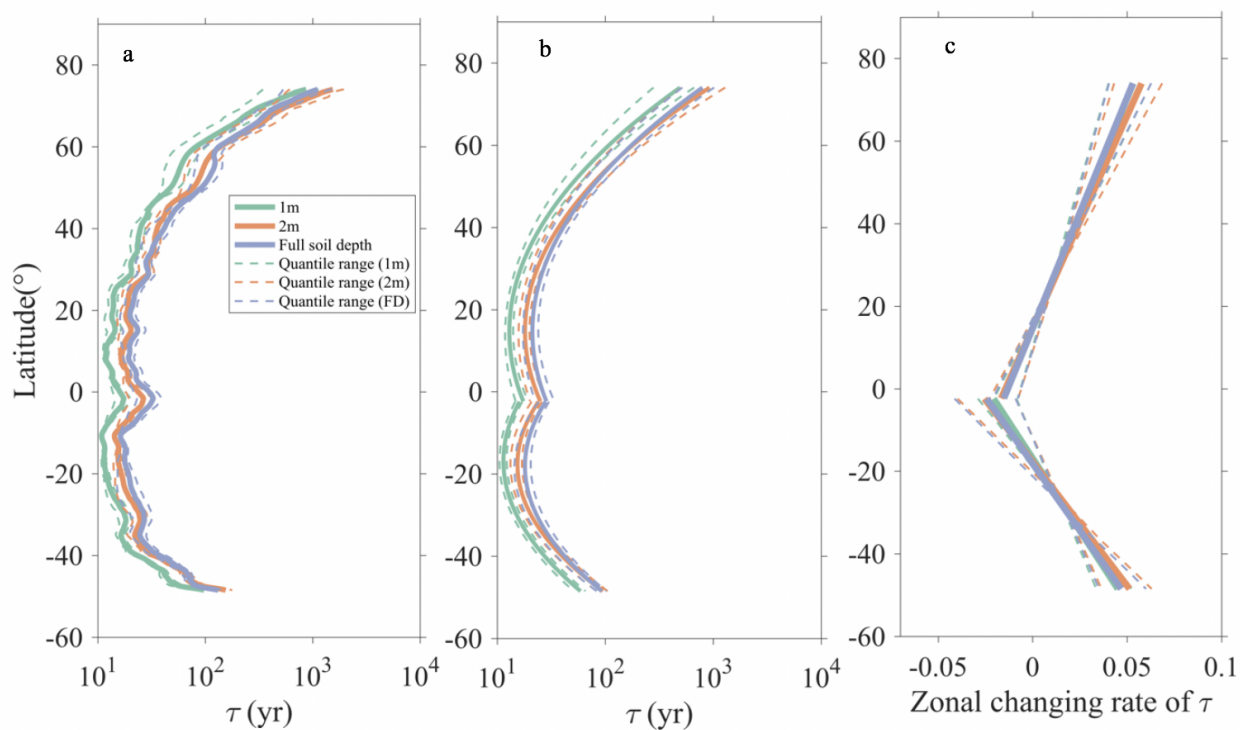

Figure 4: The contribution of τ uncertainty. Derived from difference sources of soil (0 - 2m), vegetation and GPP. Contribution from a certain variable is represented by a specific color, e.g. the green colored region indicates the uncertainty is dominated by C_{veg}.

Figure 5: (a) The zonal distribution of τ. (b) Second-degree polynomial fit. (c) Zonal change rate (first derivative of the polynomial function) of τ with latitude. Solid lines represent the mean τ for different soil depth (1m, green; 2m, red; full depth, purple) and dashed lines are the quantile range for different soil depth. The polynomial function is fitted to Northern and Southern hemisphere individually.
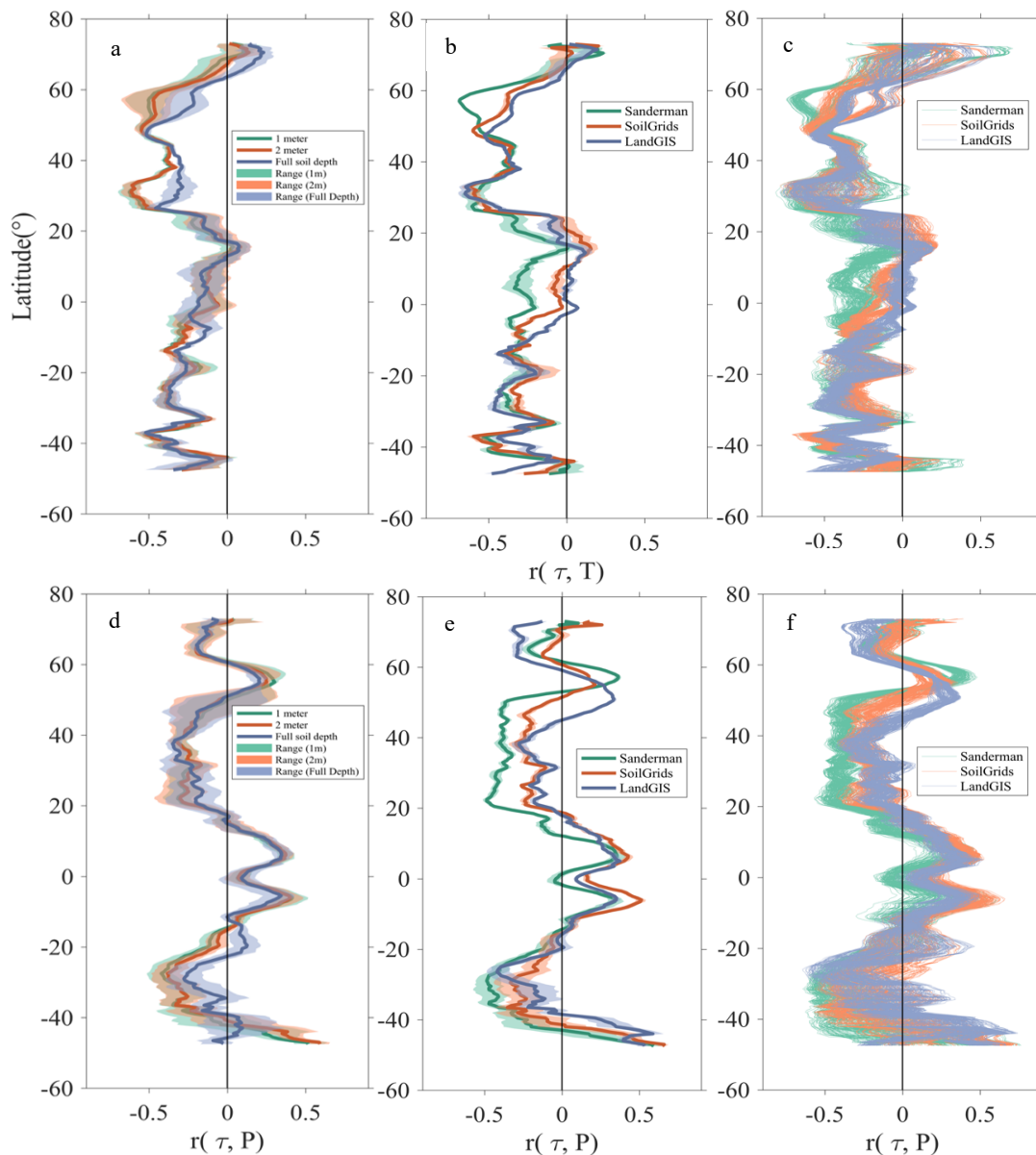
640

Figure 6: Correlation between zonal τ and Climate variables. Annual mean temperature (a, b, c) and mean annual precipitation (d, e, f) a and d colored by different soil depth (1m, green; 2m, red; full depth, purple) with shaded areas of quantile range. Subplots b and are colored by different soil source; Subplots c and f show each ensemble member and are colored by different soil data source.